Rafidain Journal of Science

https://rsci.uomosul.edu.iq

Vol. 34, No. 3, pp. 79- 90, 2025 (September)

Nonlinear Optical Properties of Pure ZnO and Sn, Al Doped and Co-Doped ZnO Thin Films Using Z-Scan Technique

Abbas A. Kareem **Yasir A. Aljawadi**

Department of Physics/ College of Sciences/ University of Mosul/ Mosul/ Iraq

Thoalfiqar A. Zaker

Department of Laser and Spectroscopy/ Laser and Photonics Centre/ University of Al-Hamdaniya/ Nineveh/ Iraq

p-ISSN: 1608-9391
e -ISSN: 2664-2786

Article information

Received: 16/2/2025
Revised: 10/4/2025
Accepted: 20/4/2025

DOI: 10.33899/rjs.2025.189220

corresponding author:
Abbas A. Kareem
abbas.sc1339@student.uomosul.edu.iq
Yasir A. Aljawadi
Yasseraljwaady@uomosul.edu.iq
Thoalfiqar A. Zaker
thoalfiqar.physics@uohamdaniya.edu.iq

ABSTRACT

The nonlinear optical (NLO) properties of pure and doped zinc oxide (ZnO) thin films, including those doped with tin (TZO), aluminum (AZO), and both aluminum and tin (ATZO), were studied using the Z-scan technique. These films were prepared using the spray pyrolysis technique. The results demonstrate that doping ZnO with aluminum (Al), tin (Sn), or both significantly influences the material's nonlinear absorption coefficient and nonlinear refractive index. Specifically, the nonlinear absorption coefficient (βeff) decreased for doped films from (5.294 cm/W) for pure ZnO film to (4.794 cm/W) for ATZO. Additionally, the nonlinear refractive index (n_2) was found to be negative for all films, were (n_2) increased from (-2.237 x 10^{-9} cm^2/W) for pure ZnO film to (-1.995 x 10^{-9} cm^2/W) for ATZO. The real, the imaginary parts of the nonlinear susceptibility and the third-order (NLO) susceptibility was also found. These results highlight how doping could improve ZnO thin film nonlinear optical performance.

Keywords: Thin films, nonlinear optical properties, Z-scan technique.

INTRODUCTION

The archetypal role of nonlinear optical (NLO) phenomena enables researchers to develop optoelectronics and photonic devices (Radhi, 2012). The relationship between matter and light produces such effects through which media reveal transformed optical characteristics (De Araújo *et al.,* 2016; Boyd, 2020). The field of laser technology alongside optical switching depends on (NLO) materials that exhibit both high nonlinear refractive (NLR) index and absorption (NLA) coefficients (Mansuripur, 2024). Nonlinear properties of transparent conductive oxides have enabled their adoption in diverse high-tech applications such as optical sensing and laser technologies and ultrafast photonics platforms (Vincenti *et al.*, 2023; Jaffray *et al.*, 2024). The implementation of transparent conductive oxides (TCOs) at a remarkable level continues in (NLO) applications. Indium tin oxide (ITO) stands as the most popular choice due to its exceptional optical nonlinearity and superior electrical and optical properties which enable its use in high-intensity laser and optoelectronic applications (Abdel-Samad *et al.*, 2024). Industrial operations that utilize indium tin oxide encounter two essential challenges namely material weakness and the scarcity of this material (Khan, 2020). The scientific community relies on aluminum zinc oxide (AZO) as a material to further understand TCOs because it shows effective high-order nonlinear frequency conversion capabilities in nanoscale applications (Jaffray *et al.*, 2024).

Researchers actively study ZnO thin films because these materials offer high optical transparency together with chemical stability and adjustable electronic and optical performance through doping with elemental additions (Özgür *et al.*, 2005; Fortunato *et al.*, 2007). A wide range of optoelectronic applications benefit from ZnO thin film exceptional qualities including solar cells (Abed *et al.*, 2016) and photodetectors (Sun *et al.*, 2010) and various innovative technological applications. The combined addition of aluminum (Al) and tin (Sn) to zinc oxide (ZnO) improves its optical characteristics to become suitable for various applications. The optical band gap rises as aluminum content increases while annealing parameters, alongside aluminum amounts, determine bandwidth assessments between 3.4 eV to 4.53 eV (Dalouji *et al.*, 2019). The combination of aluminum and tin in the material allows it to minimize ultraviolet and visible light absorption thereby increasing transparency and promoting visible light output (Guendouz *et al*., 2013; Rwenyagila *et al.*, 2014). Multilayer structures containing aluminum show short-wavelength shifts in absorption edges based on the Moss-Burstein effect (Rwenyagila *et al.*, 2014). These devices along with aluminum present better nonlinear optical properties suitable for photonic purposes and they exhibit advanced properties including nonlinear refractive index and two-photon absorption (Otieno, 2017).

The measurement of (NLO) properties involves various methods such as the Z-scan technique (Mona *et al.,* 2020; Antoine and Bonačić-Koutecký, 2018), interferometric approaches (Jansonas *et al*., 2022) and hyper-Rayleigh scattering nanomaterials (Antoine and Bonačić-Koutecký, 2018). The Z-scan technique, widely recognized for its robustness and extensive application in scientific research, is a highly efficient method for investigating the (NLO) properties of various materials by thoroughly examining their responses to laser irradiation (Badr *et al.*, 2007).

This study seeks to evaluate the (NLO) properties of pure ZnO and Sn, Al doped and co-doped ZnO thin films. For the improvement of ZnO usage in modern technological fields it is vital to conduct a detailed study and to optimize it with doping.

EXPERIMENTAL

Fig. (1) shows the Z-scan technique experimental setup used to determine the (NLO) properties. The configuration of the experimental apparatus entailed the positioning of samples upon a computer-controlled rail, which permitted meticulous adjustments along the trajectory of the laser beam and its focal point. A laser diode (A laser diode with an output power of 53 mW was used, extracted from a computer DVD player, supplied by the Japanese company (Pintel)) emitting light at a wavelength of 632.8 nm was employed, with its beam being collimated by a lens featuring

a focal length of 5 cm that was strategically located prior to the movable stage. A variable-diameter aperture was utilized to facilitate transitions between open and closed states, with the closed aperture maintained at a constant diameter of approximately 0.5 mm. At the focal point, the power of the laser beam was quantified utilizing a power meter, fixed at 0.53 x 10^2 mW ($I_O = \frac{2P}{\pi w^2} = 1.56\,x\,10^2\,MW/cm^2$). A DET10A photodetector, was employed to quantify the transmitted signal while concurrently mitigating the effects of noise and two mirrors (part No. BB1-E02-10, φ1inch) mounted on three-way moving bases were used to obtain the best laser line. The diameter of the laser beam's spot size, ascertained via the knife-edge technique, was determined to be 2.16 x 10^2 µm.

Thin films of pure zinc oxide (ZnO), as well as ZnO doped with tin (Sn), aluminum (Al), and a combination of aluminum and tin (Al-Sn), were successfully deposited on glass substrates using the spray pyrolysis method, during the deposition process, the glass substrates were heated to 400 °C.

The precursor solutions were prepared by dissolving zinc acetate $(CH_3COO)_2Zn{\cdot}2H_2O$, tin chloride $(SnCl_4{\cdot}5H_2O)$, and aluminum nitrate $(Al(NO_3)_3{\cdot}9H_2O)$ in distilled water, achieving a concentration of 0.1 M. (Table 1) summarizes the formulations of the spray solutions used for each sample.

Table 1: Labels of samples and compositions of sprayed solutions.

Designations	Sample	sprayed solutions formulations
Pure ZnO (undoped)	ZnO	100 % dissolved $(CH_3COO)_2$ Zn
Sn doped ZnO	TZO	97 % dissolved $(CH_3COO)_2$ Zn + 3 % dissolved $SnCl_4$
Al doped ZnO	AZO	97 % dissolved $(CH_3COO)_2$ Zn + 3 % dissolved $Al(NO_3)_3$
Sn-Al co-doped ZnO	ATZO	97 % dissolved $(CH_3COO)_2$ Zn + 1.5 % dissolved $SnCl_4$+ 1.5 % dissolved $Al(NO_3)_3$

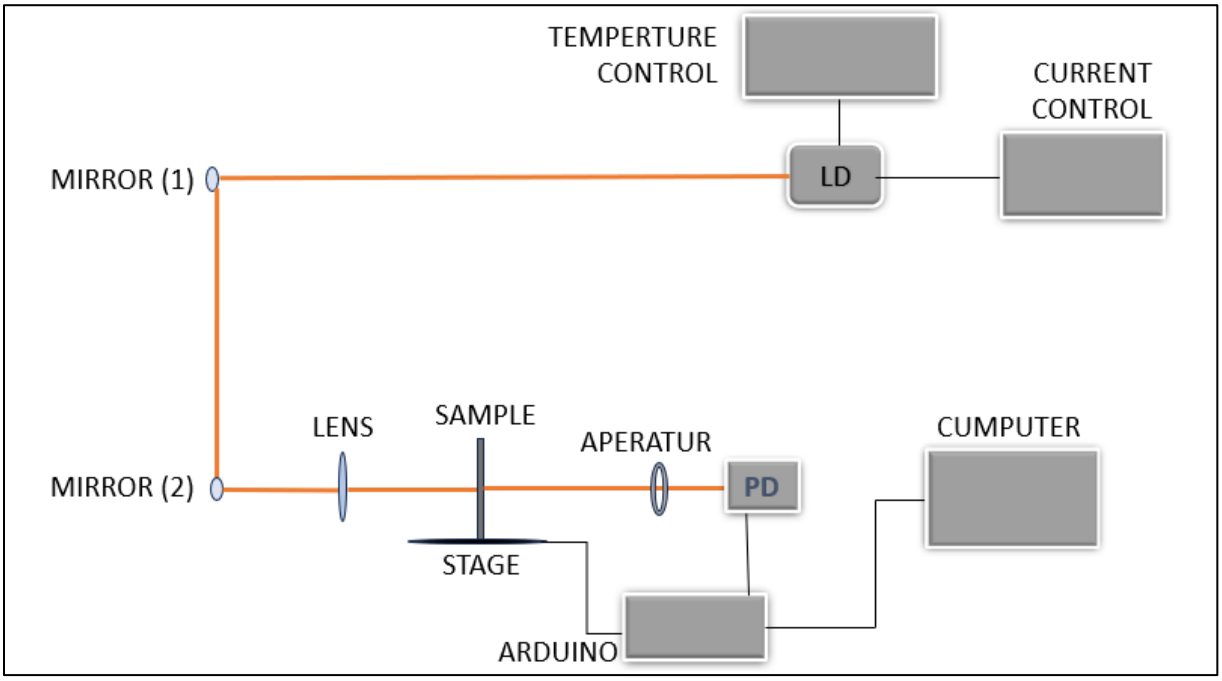

Fig. 1: Illustrates the experimental setup for Z-scan technique where LD is (Laser diode) and PD is (Photodetector).

RESULTS AND DISSECTION

The open aperture was used to measure nonlinear absorption coefficient (*βeff*), Fig. (2) shows the normalized transmittance curve as a function of the position on the Z-axis for pure ZnO using open aperture, where the valley shape indicates a decrease in transmittance at the focal point (Z=0), followed by a gradual increase as the position moves away from the focal point in both the positive and negative Z directions. The value of (*βeff*) is found to be 5.294 cm/W as shown in (Table 2). Various nonlinear phenomena may account for this specific type of absorption, including two-photon absorption (TPA), nonlinear scattering, free-carrier absorption (FCA), as well as the interplay of these mechanisms. Indicating (TPA) effects play a significant role in the optical response of the material (Chacko *et al.,* 2006; Banyamin *et al.*, 2014; Ismail *et al.,* 2025).

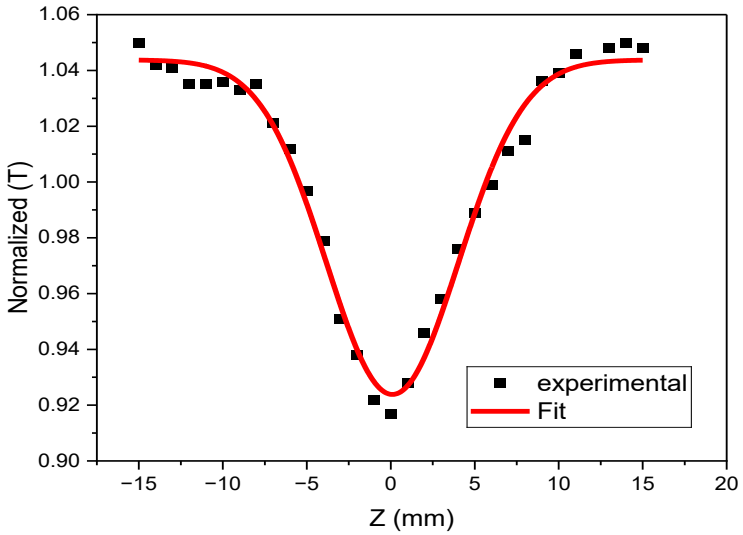

Fig. 2: Illustrates the normalized transmittance of pure ZnO measured using open aperture setup.

Fig. (3) shows the normalized transmittance curve as a function of the position on the Z-axis for Al doped ZnO (AZO), the value of (*βeff*) decreased as shown in (Table 2) compared to ZnO film. When zinc oxide is doped with aluminum, the number of free carriers in the material increases, which reduces nonlinear effects such as (TPA), thus lowering the (*βeff*). The effective nonlinear refractive index (*β*eff) in Al-doped ZnO (AZO) decreases compared to pure ZnO due to the increased concentration of free carriers introduced by aluminum doping. This phenomenon is supported by several studies that explore the impact of Al doping on ZnO's optical properties. Aluminum atoms replace some zinc ions in the crystal lattice, adding extra electrons to the material, which increases the number of free carriers and reduces nonlinear optical effects like two-photon absorption (TPA). The increased free carriers absorb and scatter photons, thereby lowering the intensity of nonlinear interactions. Additionally, the increased free carriers screen Coulomb interactions between charged particles, weakening the nonlinear effects (Otieno, 2017). The refractive index of the material also changes with doping, typically decreasing with higher carrier concentrations, which further contributes to the reduction of *β*eff (Khudhr and Abass, 2016). In pure ZnO, the lower carrier concentration enhances the nonlinear effects, resulting in a higher *β*eff (Otieno, 2017). However, when aluminum is doped into ZnO, the increased number of free carriers weakens the nonlinear effects, leading to a reduction in *β*eff, as observed in various studies (Otieno, 2017; Kovalenko *et al.*, 2021). Therefore, doping ZnO with aluminum significantly influences its nonlinear optical properties, primarily by decreasing TPA, which results in a lower effective nonlinear refractive index. This is consistent with the observed changes in optical properties such as increased transmittance and decreased absorption with higher Al doping levels (Khudhr and Abass, 2016; Kovalenko *et al.*, 2021).

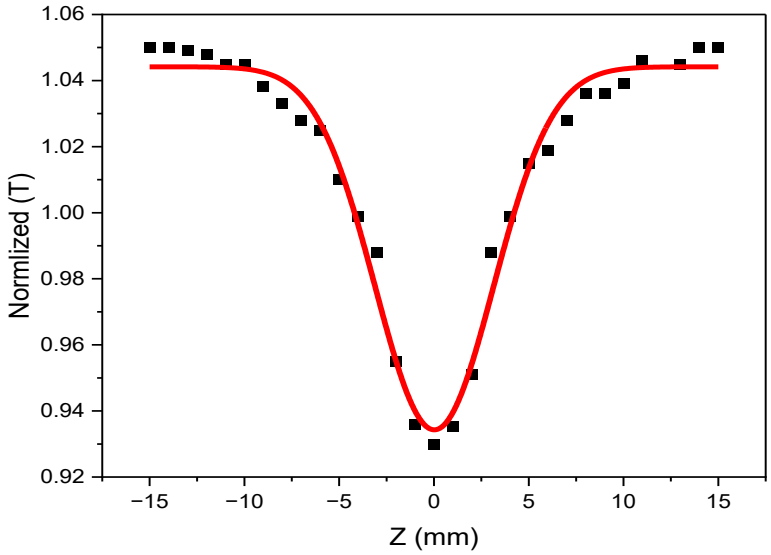

Fig. 3: Illustrates the normalized transmittance of Al doped ZnO (AZO) measured using open aperture setup.

Fig. (4) shows the normalized transmittance curve as a function of the position on the Z-axis for Sn doped ZnO (TZO), the value of (*βeff*) decreased as shown in (Table 2) compared to ZnO film and AZO. When zinc oxide is doped with tin, a similar change occurs as with aluminum doping, where the number of free carriers in the material increases, reducing nonlinear effects such as (TPA), thus lowering the (*βeff*).

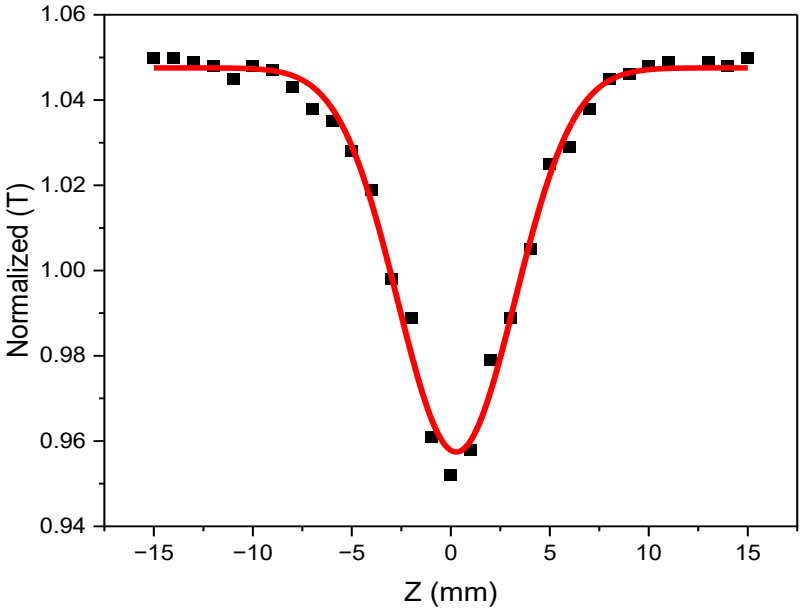

Fig. 4: Illustrates the normalized transmittance of Sn doped ZnO (TZO) measured using open aperture setup.

Fig. (5) shows the normalized transmittance curve as a function of the position on the Z-axis for Al-Sn codoped ZnO (ATZO), the value of (*βeff*) decreased as shown in (Table 2). When zinc oxide is doped with both aluminum and tin simultaneously, a combined effect occurs, increasing the number of free carriers in the material, which reduces nonlinear effects such as (TPA), thus lowering the (*βeff*).

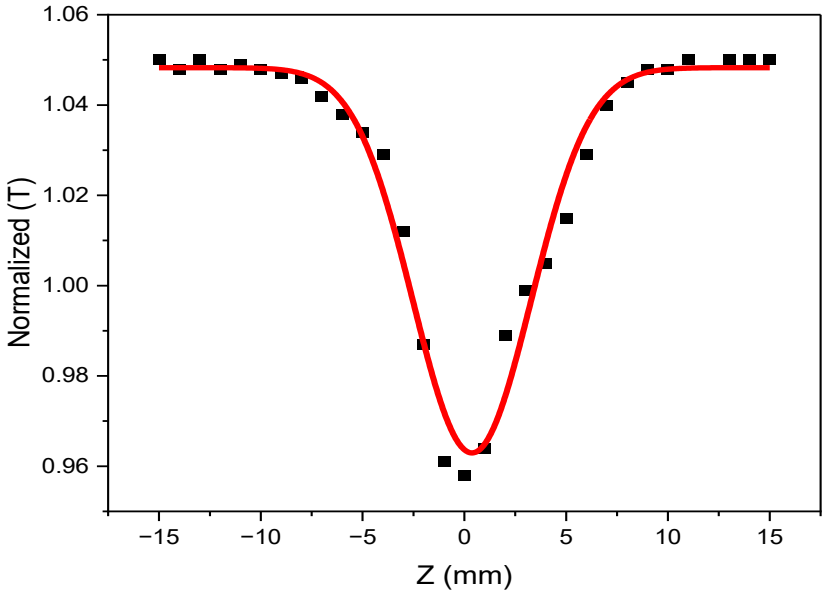

Fig. 5: Illustrates the normalized transmittance of Al, Sn co-doped ZnO (ATZO) measured using open aperture setup.

The value of TPA coefficient can be obtained through fitting the open aperture measurements using the subsequent equation (Ismail *et al.,* 2025):

$$T(Z) = 1 - \left[\frac{\beta_{eff} I_o L_{eff}}{2\sqrt{2}\left(1 + \frac{Z^2}{Z_o^2}\right)}\right] \ldots\ldots (1)$$

Where, Z is the distance between the focus and the sample, L_{eff} is the effective length ($L_{eff} = \frac{1-e^{-\alpha L}}{\alpha}$), Z_o is the Rayleigh range ($Z_o = \frac{\pi\omega_o^2}{\lambda}$) and I_o is the laser intensity at the focal ($I_o = \frac{2P}{\pi\omega_o^2}$) . Where the parameters α, L, ω_0 and P refers to linear absorption coefficient determined using spectrophotometer at wavelength (λ=632.8 nm), thickness of the samples, the waist length and the laser power respectively.

The close aperture was used to measure (n_2) dependent on the variation between the intensity the peak and that of the valley, as shown in the subsequent equation (Ismail *et al.,* 2025);

$$n_2 = \left(\frac{1}{0.405(1-S)^{0.25} K I_o L_{eff}} \Delta T_{P-v}\right) \ldots\ldots (2)$$

Where ($S = 1 - e^{-\frac{2r^2}{\omega^2}}$) can be determined dependent on the aperture and diameters of the beam while K is the wavenumber.

A negative refractive index occurs when the nonlinear refractive index n_2 becomes negative, causing self-defocusing behavior. This can happen due to the Kerr effect, where the refractive index changes with light intensity, or due to thermal effects that alter the refractive index through local heating. In ZnO, a negative n_2 results in a peak before the focal point and a valley after, as observed in the Z-scan measurements. Other factors like electro strictive effects or mechanical influences may also contribute, but thermal and Kerr effects are the primary causes (Bongu *et al.*, 2023).

Fig. (6) presents Z-Scan measurements of a pure zinc oxide (ZnO) layer using the closed-aperture setup. The horizontal axis represents the position along the Z-axis (mm), while the vertical axis corresponds to the normalized transmittance. The curve exhibits a peak before the focal point (Z<0), followed by a valley after the focal point (Z>0), indicating a negative phase shift. This suggests that the material has a negative (n_2) (n_2<0) and, consequently, exhibits self-defocusing behavior (Bairy *et al.*, 2019).

Moreover, the distance between the peak and the valley exceeds the Rayleigh length (Z_0). The (NLR) index within a material may arise from a multitude of mechanisms, encompassing solely electronic phenomena (Kerr effect), thermal effects, electro-strictive interactions, mechanical influences, among others (Romaniuk, 2007). Indicating that thermal nonlinear effects play a significant role in the optical response of the material (Ayana *et al.*, 2024). The value of (n_2) is found to be (-2.237x 10^{-9} cm/W) as shown in (Table 2).

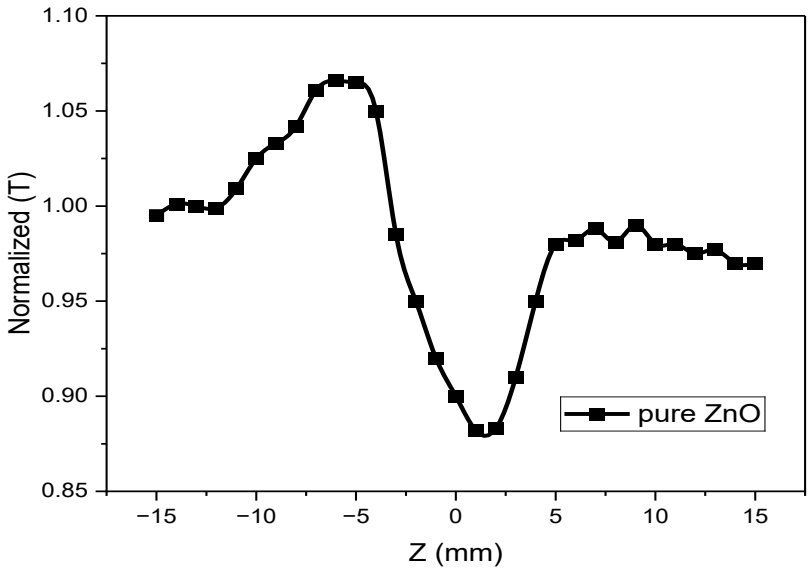

Fig. 6: Illustrates the normalized transmittance of pure ZnO measured using close aperture setup.

Fig. (7) presents the normalized transmittance curve for AZO as a function of the Z-axis position in the closed-aperture setup. The curve exhibits a peak before the focal point (Z<0) and a valley after it (Z>0), indicating a negative phase shift. The (n_2) for AZO was found to be (-2.201×10^{-9} cm^2/W), which is slightly higher than that of pure ZnO as shown in (Table 2). This increase in (n_2) suggests that adding aluminum leads to changes in the material's structure, reducing its ability to interact non-linearly with light and leading to enhanced (NLO) properties. Like ZnO, AZO exhibits self-defocusing behavior due to its negative (n_2) value.

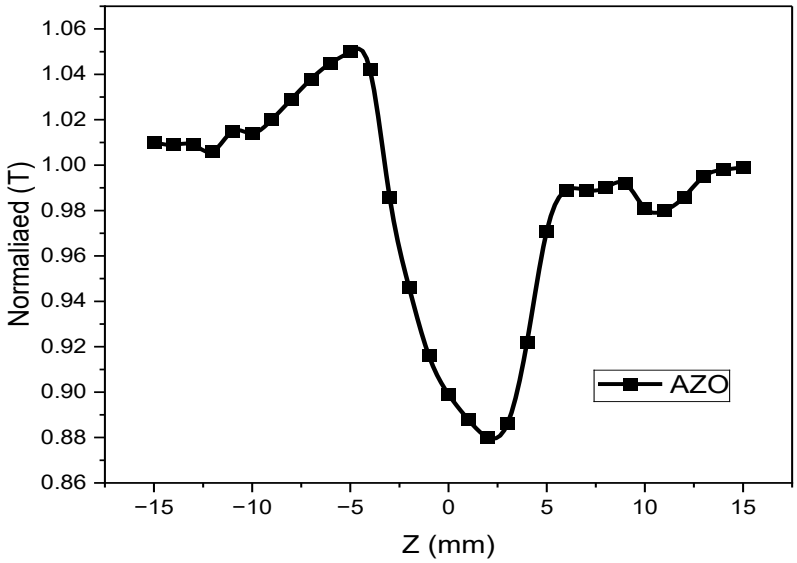

Fig. 7: Illustrates the normalized transmittance of Al doped ZnO (AZO) measured using close aperture setup.

Fig. (8) illustrates the normalized transmittance curve for (TZO), showing a similar pattern with a peak before the focal point and a valley after it, signifying a negative phase shift. The (n_2) for TZO is measured as (-2.154) × 10^{-9} cm^2/W, which is higher than that of ZnO as shown in (Table 2) but slightly lower than AZO. This increase in (n_2) suggests that adding tin leads to changes in the material's structure, reducing its ability to interact non-linearly with light and leading to enhanced (NLO) properties. Like ZnO, (TZO) exhibits self-defocusing behavior due to its negative (n_2) value.

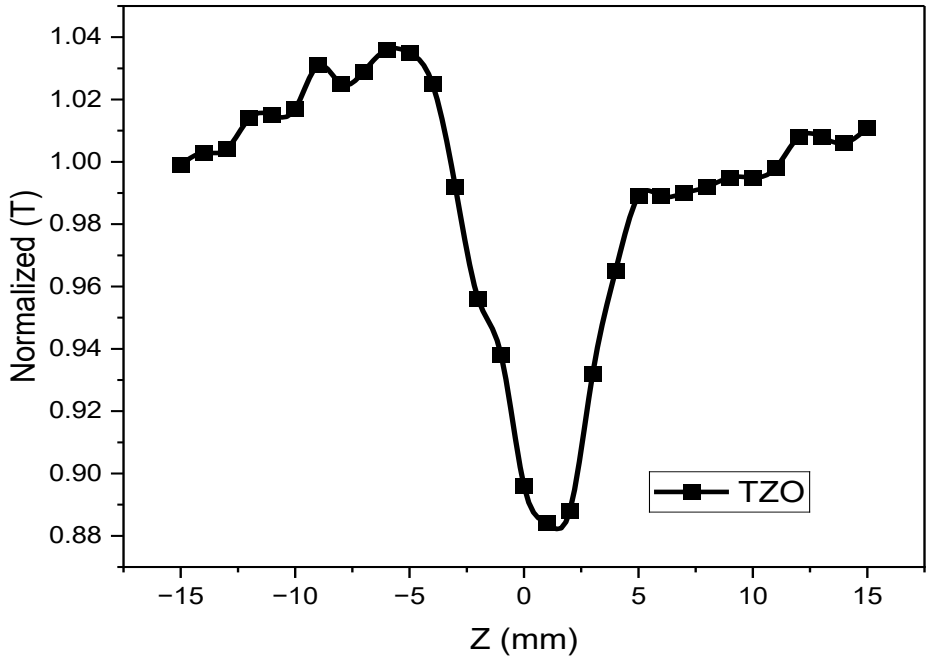

Fig. 8: Illustrates the normalized transmittance of Sn doped ZnO (TZO) measured using close aperture setup.

Fig. (9) shows the normalized transmittance curve for (ATZO), following the same self-defocusing trend observed in (AZO) and TZO. The (n_2) for ATZO is recorded as (-1.995×10^{-9} cm^2/W), which, while still negative, is Higher than both (AZO) and (TZO) as shown in (Table 2). This reduction in magnitude suggests that co-doping with aluminum and tin results in structural modifications that slightly decrease the material's ability to interact non-linearly with light.

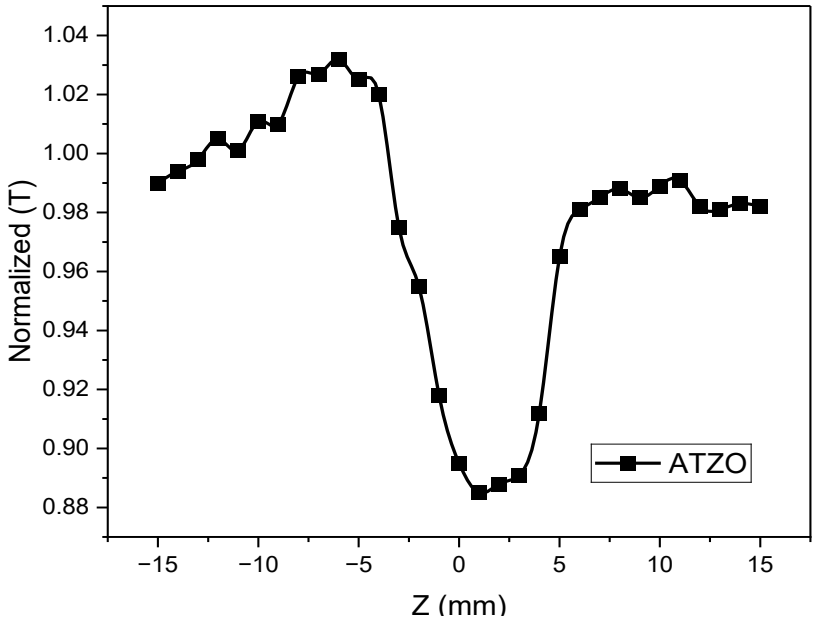

Fig. 9: Illustrates the normalized transmittance of Al, Sn co-doped ZnO (ATZO) measured using close aperture setup.

The absolute value, along with the real and imaginary parts of the nonlinear susceptibility, can be determined by substituting n_2 and *βeff* into the following equations (Zidan and Allahham, 2015):

$$ReX^{(3)}(esu) = 10^{-4} x \frac{\varepsilon_o c^2 n_o^2 n_2}{\pi} \left(\frac{cm^2}{w}\right) \ldots\ldots (3)$$

$$ImX^{(3)}(esu) = 10^{-2} x \frac{\varepsilon_o c^2 n_o^2 \lambda \beta_{eff}}{4\pi^2} \left(\frac{cm}{w}\right) \ldots\ldots (4)$$

Where n_o represents the linear refractive index of the material, $\boldsymbol{\varepsilon}_o$ denotes the permittivity of vacuum, and c refers to the speed of light in vacuum.

The third-order (NLO) susceptibility can be determined using the subsequent equation (Zidan and Allahham, 2015).

$$|\chi^3| = \sqrt{(ReX^{(3)})^2 + (ImX^{(3)})^2}(esu) \ldots (5)$$

Table 2: The nonlinear optical parameters pure ZnO, Al-Sn doped and co-doped ZnO.

Sample	*βeff* cm/W	n_2 x 10^{-9} cm^2/W	$ReX^{(3)}$(esu)	$ImX^{(3)}$ (esu)	$\lvert\chi^3\rvert$ (esu)
Pure ZnO	5.294	-2.237	-0.00324	0.262	0.273
AZO	5.107	-2.201	-0.00312	0.214	0.226
TZO	4.853	-2.142	-0.00274	0.165	0.178
ATZO	4.794	-1.995	-0.00223	0.152	0.161

According to the results obtained from the above table, it is suitable for various nonlinear optical applications such as optoelectronic devices, optical switching and frequency conversion (Ganesh *et al.,* 2017; Ayana *et al.,* 2024).

CONCLUSIONS

The study investigates the (NLO) properties of pure ZnO and Sn, Al doped and co-doped ZnO thin films, using the Z-scan technique. These films were prepared using the spray pyrolysis technique. The results demonstrate that doping ZnO with aluminum, tin, or both significantly influences the material's nonlinear absorption and refractive index. Specifically, the (β_{eff}) decreased for doped films from (5.294) cm/W for ZnO film to (5.107, 4.853 and 4.794) cm/W for AZO, TZO and ATZO respectively, attributed to the increased number of free carriers in the material, which reduces nonlinear effects like (TPA) and these results leading to enhanced (NLO) properties. Additionally, the (n_2) was found to be negative for all films, indicating self-defocusing behavior, Additionally, the nonlinear refractive index (n_2) was found to be negative for all films, indicating self-defocusing behavior, were (n_2) increased from (-2.237) x 10^{-9} cm^2/W for ZnO film to (-2.201, -2.154 and -1.995) x 10^{-9} cm^2/W for AZO, TZO and ATZO respectively and these results leading to enhanced (NLO) properties. The real parts decreased and imaginary parts increased of the nonlinear susceptibility for dopant films, while the third-order (NLO) susceptibility decreased for dopant films.

REFERENCES

Abdel-Samad, F.; Mahmoud, A.; Mohamed, T.A. (2024). A comprehensive review of nonlinear optical properties of ITO semiconductor material. *Lira J.*, **2**(1), 1-42. DOI:10.21608/lira.2024.357508

Abed, S.; Bouchouit, K.; Aida, M.S.; Taboukhat, S.; Sofiani, Z.; Kulyk, B.; Figa, V. (2016). Nonlinear optical properties of zinc oxide doped bismuth thin films using Z-scan technique. *Opt. Mat.*, **56**, 40-44. DOI:10.1016/j.optmat.2015.12.014

Antoine, R.; Bonačić-Koutecký, V. (2018). "Measurement Techniques of Optical Nonlinearities-Two-Photon Absorption/Fluorescence and Hyper-Rayleigh Scattering". Springer, pp.49-62. DOI:10.1007/978-3-319-64743-2_6

Ayana, A.; Gummagol, N.B.; Patil, P.S.; Sharma, P.; Rajendra, B.V. (2024). Nonlinear optical properties of zinc oxide thin films. *Opt. Laser Tech.,* **175**, 110820. DOI:10.1016/j.optlastec.2024.110820

Badr, B.A.M.; Hamadi, O.A.; Yousif, A.K. (2007). Measurement of thermos optic coefficient in lead sulfide using laser single-beam scanning technique. *Eng. Tech. J.*, **25**(5).

Bairy, R.; Patil, P.S.; Maidur, S.R.; Vijeth, H.; Murari, M.S.; Bhat, U.K. (2019). The role of cobalt doping in tuning the band gap, surface morphology, and third-order optical nonlinearities of ZnO nanostructures for NLO device applications. *RSC Adv.,* **9**(39), 22302-22312. DOI:10.1039/c9ra03006a

Banyamin, Z.; Kelly, P.; West, G.; Boardman, J. (2014). Electrical and optical properties of fluorine-doped tin oxide thin films prepared by magnetron sputtering. *Coat.*, **4**(4), 732-746. DOI:10.3390/coatings4040732

Bongu, S.R.; Buchmüller, M.; Neumaier, D.; Görrn, P. (2023). Electric control of thermal contributions to the nonlinear optical properties of nitrobenzene. *Adv. Phy. Res*., DOI:10.1002/apxr.202300053

Boyd, R.W. (2020). "Nonlinear Optics". 3rd ed., Elsevier, Academic Press.

Chacko, S.; Bushiri, M.J.; Vaidyan, V.K. (2006). Photoluminescence studies of spray pyrolytically grown nanostructured tin oxide semiconductor thin films on glass substrates. *J. Phy. D: App. Phy.*, **39**(21), 4540-4543. DOI:10.1088/0022-3727/39/21/004

Dalouji, V.; Ebrahimi, P.; Binaei, N.; Tanhaee, E.; Nezafat, N.B.; Dejam, L.; Solaymani, S. (2019). The optical properties of aluminum-doped zinc oxide thin films (AZO): New methods for estimating gap states and non-linear properties. *Mat. Chem. Phy.,* **236**, 121842. DOI:10.1016/j.matchemphys.2019.121842

De Araújo, C.B.; Gomes, A.S.; Boudebs, G. (2016). Techniques for nonlinear optical characterization of materials: A review. *Rep. Pro. Phy.,* **79**(3), 036401. DOI:10.1088/0034-4885/79/3/036401

Fortunato, E.; Ginley, D.; Hosono, H.; Paine, D.C. (2007). Transparent conducting oxides for photovoltaics. *MRS Bull.,* **32**(3), 242-247. DOI:10.1557/mrs2007.29

Ganesh, V.; Yahia, I. S.; AlFaify, S.; Shkir, M. (2017). Sn-doped ZnO nanocrystalline thin films with enhanced linear and nonlinear optical properties for optoelectronic applications. *J. Phy. Chem. Solids*, **100**, 115-125. DOI:10.1016/j.jpcs.2016.09.022

Guendouz, H.; Bouaine, A.; Brihi, N. (2021). Ultrawide bandgap high near ultraviolet transparency amorphous Sn-Al co-doped ZnO thin films. *J. Non-Cryst. Solids*, **569**, 121001. DOI:10.1016/J.JNONCRYSOL.2021.121001

Ismail, F.I.; Zakar, A.T.; Zaker, T.A. (2025). Effect of aluminum doping on structural and nonlinear optical properties of tin dioxide films prepared by spray pyrolysis. *Iraqi J. App. Phy*., **21**(1), 93-100.

Jaffray, W.; Belli, F.; Stengel, S.; Vincenti, M.A.; Scalora, M.; Clerici, M.; Шалаев, В.И.; Boltasseva, A.; Ferrera, M. (2024). High-order nonlinear frequency conversion in transparent conducting oxide thin films. *Adv. Opt. Mat*., DOI:10.1002/adom.202401249

Jansonas, G.; Budriūnas, R.; Vengris, M.; Varanavičius, A. (2022). Interferometric measurements of nonlinear refractive index in the infrared spectral range. *Opt. Exp*., **30**(17), 30507-30524. DOI:10.1364/OE.458850

Khan, A. (2020). Introduction to transparent conductors. In: Novel embedded metal-mesh transparent electrodes. Springer Theses. Springer, Singapore., 1-8. DOI:10.1007/978-981-15-2918-4_1

Khudhr, M.M.; Abass, K.H. (2016). Effect of al-doping on the optical properties of ZnO thin film prepared by thermal evaporation technique. *Inter. J. Eng*., **7**, 25-31. DOI:10.18052/WWW.SCIPRESS.COM/IJET.7.25

Kovalenko, M.; Bovgyra, O.V.; Dzikovskyi, V.; Kashuba, A.I.; Ilchuk, H.A.; Petrus, R.; Semkiv, I.V. (2021). Effect of Al doping on optical properties of ZnO thin films: Theory and experiment. *Phy. Chem. Solid State*, **22**(1), 153-159. DOI:10.15330/PCSS.22.1.153-159

Mansuripur, M. (2024). Fundamental principles and applications of nonlinear optical phenomena in classical and quantum electrodynamics. *Proc. SPIE*, **13126**, 1312605. DOI:10.1117/12.3028528

Mona, A.; Abdullah, S.; Mohamed, B.A.; Ashour, W.Z.; Tawfik, R.; Schuch, R.; Mohamed, T. (2020). Measuring the nonlinear optical properties of indium tin oxide thin film using femtosecond laser pulses. *J. Opt. Soc. America B*, **37**(11). DOI:10.1364/JOSAB.396327

Otieno, C.O. (2017). Nonlinear optical properties of aluminum doped zinc oxide. Doctoral dissertation, ProQuest, State University of New York at Binghamton.

Özgür, Ü.; Alivov, Y.I.; Liu, C.; Teke, A.; Reshchikov, M.A.; Doğan, S.; Avrutin, V.; Cho, S.-J.; Morkoç, H. (2005). A comprehensive review of ZnO materials and devices. *J. App. Phy.,* **98**(4), 041301. DOI:10.1063/1.1992666

Radhi, F.S. (2012). Nonlinear responses and optical limiting behavior of 2-Chloro-5-nitroanisole dye under CW laser illumination. *J. Kerbala Uni*., **8**(2), 181-186.

Romaniuk, R.S. (2007). Non-linear glasses and metaglasses for photonics, a review: Part II. Kerr nonlinearity and metaglasses of positive and negative refraction. *SPIE,* **6937**, 693717. DOI:10.1117/12.784672

Rwenyagila, E.R.; Agyei-Tuffour, B.; Zebaze Kana, M.G.; Akin-Ojo, O.; Soboyejo, W.O. (2014). Optical properties of ZnO/Al/ZnO multilayer films for large area transparent electrodes. *J. Mat. Res.*, **29**(24), 2912-2920. DOI:10.1557/jmr.2014.298

Sun, J.; Dai, Q.; Liu, F.; Huang, H.; Li, Z.; Zhang, X.; Wang, Y. (2010). The ultraviolet photoconductive detector based on Al-doped ZnO thin film with fast response. *Sci. China Phy. Mech. Astro.,* **54**(1), 102-105. DOI:10.1007/s11433-010-4203-y

Vincenti, M.A.; de Ceglia, D.; Scalora, M. (2023). Harmonic generation in transparent conducting oxides: From nanolayers to multilayers and photonic crystal arrangements. *Metamat.*, X- 411. DOI:10.1109/metamaterials58257.2023.10289385

Zidan, M.D.; Allahham, A. (2015). Z-Scan measurements of the third-order optical nonlinearity of a C60 doped poly (dimethylacetylendicarboxylate). *Acta Phy. Pol. A,* **128**(1), 25. DOI:10.12693/APhysPolA.128.25

الخصائص البصرية غير الخطية لأغشية ZnO المطعم بـ Al و Sn بشكل أحادي ومزدوج باستخدام تقنية Z-scan

عباس عبد الرزاق كريم **ياسر عبد الجواد الجوادي**

قسم الفيزياء/ كلية العلوم/ جامعة الموصل/ الموصل/ العراق

ذو الفقار علي زكر

قسم الليزر والأطياف/ مركز الليزر والفوتونيات/ جامعة الحمدانية/ نينوى/ العراق

الملخص

تمت دراسة الخصائص البصرية غير الخطية (NLO) لأغشية أكسيد الزنك (ZnO) الرقيقة النقية والمطعمة، بما في ذلك الأغشية المطعمة بالقصدير (TZO) والألمنيوم (AZO) وكلاهما معًا (ATZO)، باستخدام تقنية المسح على شكل Z. تم تحضير هذه الأغشية باستخدام تقنية التحلل الحراري بالرش. أظهرت النتائج أن تطعيم ZnO بالألمنيوم (Al) أو القصدير (Sn) أو كليهما له تأثير كبير على معامل الامتصاص غير الخطي ومعامل الانكسار غير الخطي للمادة. حيث انخفض معامل الامتصاص غير الخطي (*βeff*) في الأغشية المطعمة من 5.294 سم/واط للأغشية النقية إلى 4.794 سم/واط لأغشية ATZO. بالإضافة إلى ذلك، وُجد أن معامل الانكسار غير الخطي (n_2) كان سالبًا في جميع الأغشية، حيث ازداد من (-2.237×10^{-9} سم²/واط) لأغشية ZnO النقية إلى (-1.995×10^{-9} سم²/واط) لأغشية ATZO. كما تم تحديد الأجزاء الحقيقية والتخيلية من القابلية غير الخطية، بالإضافة إلى القابلية غير الخطية من الرتبة الثالثة. تبرز هذه النتائج كيف يمكن للتطعيم أن يحسن أداء الأغشية الرقيقة لأكسيد الزنك في الخصائص البصرية غير الخطية.

الكلمات الدالة: اغشية رقيقة، الخصائص البصرية غير الخطية، تقنية Z-scan.